

Iminoribitol Transition State Analogue Inhibitors of Protozoan Nucleoside Hydrolases[†]

Robert W. Miles,[‡] Peter C. Tyler,[§] Gary B. Evans,[§] Richard H. Furneaux,[§] David W. Parkin,^{§,||} and Vern L. Schramm^{*,‡}

Department of Biochemistry, Albert Einstein College of Medicine, Bronx, New York 10461, and Carbohydrate Chemistry Team, Industrial Research Limited, Lower Hutt, New Zealand

Received April 9, 1999; Revised Manuscript Received July 29, 1999

ABSTRACT: Nucleoside *N*-ribohydrolases from protozoan parasites are targets for inhibitor design in these purine-auxotrophic organisms. Purine-specific and purine/pyrimidine-nonspecific nucleoside hydrolases have been reported. Iminoribitols that are 1-substituted with meta- and para-derivatized phenyl groups [(1*S*)-substituted 1,4-dideoxy-1,4-imino-*D*-ribitols] are powerful inhibitors for the nonspecific nucleoside *N*-ribohydrolases, but are weak inhibitors for purine-specific isozymes [Parkin, D. W., Limberg, G., Tyler, P. C., Furneaux, R. H., Chen, X.-Y., and Schramm, V. L. (1997) *Biochemistry* 36, 3528–3534]. Binding of these inhibitors to nonspecific nucleoside hydrolase occurs primarily via interaction with the iminoribitol, a ribooxocarbenium ion analogue of the transition state. Weaker interactions arise from hydrophobic interactions between the phenyl group and the purine/pyrimidine site. In contrast, the purine-specific enzymes obtain equal catalytic potential from leaving group activation and ribooxocarbenium ion formation. Knowledge of the reaction mechanisms and transition states for these enzymes has guided the design of isozyme-specific transition state analogue inhibitors. New synthetic efforts have produced novel inhibitors that incorporate features of the leaving group hydrogen-bonding sites while retaining the iminoribitol group. These compounds provide the first transition state analogue inhibitors for purine-specific nucleoside hydrolase. The most inhibitory 1-substituted iminoribitol heterocycle is a sub-nanomolar inhibitor for the purine-specific nucleoside hydrolase from *Trypanosoma brucei brucei*. Novel nanomolar inhibitors are also described for the nonspecific nucleoside hydrolase from *Crithidia fasciculata*. The compounds reported here are the most powerful iminoribitol inhibitors yet described for the nucleoside hydrolases.

Nucleoside *N*-ribohydrolases are widely distributed in bacteria, yeast, and protozoa but are not found in mammals (1, 2). These enzymes catalyze hydrolysis of the *N*-ribosidic bond of purine and pyrimidine nucleosides:



Nonspecific nucleoside hydrolases (NNHs) catalyze hydrolysis of natural purine and pyrimidine nucleosides and also hydrolyze the O-linked *p*-nitrophenyl β -*D*-ribofuranoside at even more efficient catalytic rates. In contrast, the specific nucleoside hydrolases (SNHs) prefer purine nucleosides and are poor catalysts for either pyrimidine nucleosides or *p*-nitrophenyl β -*D*-ribofuranoside (3–6). This difference in substrate specificity can be rationalized in terms of the possible enzymatic mechanisms of *N*-riboside hydrolysis, which include (1) leaving group assistance, (2) ribooxocarbenium ion stabilization, and (3) water activation (7). The *p*-nitrophenyl substituent is a good leaving group, requiring

no activation, and has a pK_a value that is too low to permit protonation by an enzymatic general acid. The nonspecific enzymes efficiently hydrolyze *p*-nitrophenyl β -*D*-ribofuranoside because they use ribooxocarbenium ion stabilization as the major contributor to catalysis. Since purine-specific nucleoside hydrolases rely more on leaving group protonation than on sugar activation, they are poor catalysts for *p*-nitrophenyl β -*D*-ribofuranoside hydrolysis. Thus, the general acids that protonate the purine leaving group play an important role in transition state stabilization of SNHs (5, 6).

Our prototype for the NNHs is the inosine-uridine nucleoside hydrolase (IU-NH) from *Crithidia fasciculata* (8, 9). Of the 17.7 kcal/mol that IU-NH provides to lower the activation energy for inosine hydrolysis, 13.1 kcal/mol is involved in ribosyl activation, and the remaining 4.6 kcal/mol stems from leaving group assistance (10). Specific inhibitors for IU-NH were designed to take advantage of this energy partition by incorporating an iminoribitol sugar in place of ribose and a substituted phenyl ring in place of the natural heterocycle. As expected, these compounds bound poorly to an SNH (11). Key features of the X-ray crystal structure of IU-NH with *p*-aminophenyl-(1*S*)-iminoribitol (12) corroborate the importance of ribosyl activation in NNHs: (1) anchoring of the C5' hydroxyl in an optimal orientation for oxocarbenium ion stabilization, (2) direct

[†] Supported by Grant GM41916 from the National Institutes of Health.

^{*} Corresponding author. Telephone: (718) 430-2813. Fax: (718) 430-8565. E-mail: vern@aecom.yu.edu.

[‡] Albert Einstein College of Medicine.

[§] Industrial Research Limited.

^{||} Present address: Department of Biochemistry, University of Dundee, Dundee DD1 4HN, Scotland.

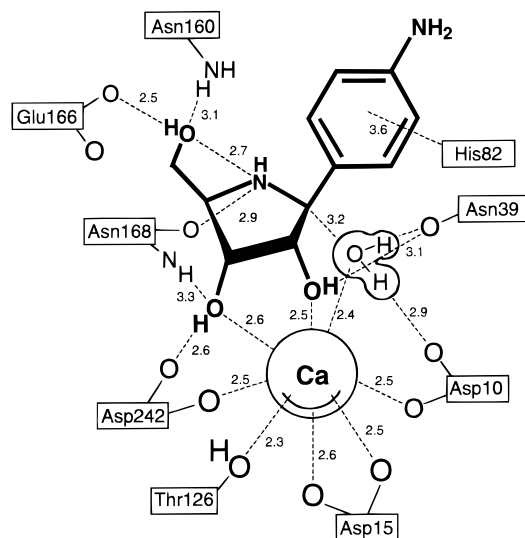


FIGURE 1: Contacts between pAPIR and IU-NH (20). The distances are in angstroms; all contacts between the enzyme and inhibitor that are ≤ 3.1 Å long are included except Asp14–O2'. Other selected distances are interactions with the leaving group and the water nucleophile.

chelation of both C2' and C3' hydroxyls with an enzyme-bound Ca^{2+} to position the sugar in a favorable geometry for oxocarbenium ion stabilization, and (3) hydrogen bonding of an imino hydrogen to enzymatic groups that may electrostatically stabilize the transition state oxocarbenium ion (Figure 1). The only proposed leaving group interaction, protonation of N7 by His241 (in purine substrates), cannot be verified from the crystal structure with *p*-aminophenyl-(1*S*)-iminoribitol (10, 12, 13).

Our prototype for the SNHs is the inosine-adenosine-guanosine nucleoside hydrolase (IAG-NH) from *Trypanosoma brucei brucei* (5, 14). This nucleoside hydrolase derives equal energetic contributions from leaving group activation (8.8 kcal/mol) and ribooxocarbenium ion stabilization (8.9 kcal/mol) (11). No structural information is available for IAG-NH; however, pH profiles indicate two general acids on the enzyme that must be protonated for optimal activity (5). Yet unlike the case for the IU-NH enzyme, no transition state inhibitors have been reported for IAG-NH.

The challenge is to use information about the catalytic mechanism to design (1) tight-binding inhibitors for an SNH (IAG-NH), (2) inhibitors specific for an SNH (IAG-NH) or for an NNH (IU-NH), and (3) nonspecific inhibitors capable of binding both isozymes. Design of SNH-specific inhibitors capitalizes on the catalytic machinery for base activation by incorporating structural features in the inhibitor that imitate the aglycon portion of the transition state in both position and pK_a . Inhibitors designed in this way are expected to have molecular electrostatic potential surfaces more closely related to an SNH transition state than to that of NNH. Matching the molecular electrostatic potential features of the transition state in inhibitor design is a significant achievement, since molecular electrostatic potential mapping is the most definitive approach for obtaining transition state inhibitors (9, 15). Although the transition states of all known nucleoside hydrolases are ribooxocarbenium ion in character, the isozyme differences in leaving group and ribooxocarbenium interaction energies provide an approach to inhibitor specificity.

Novel iminoribitol compounds that powerfully inhibit (nanomolar to sub-nanomolar) IU-NH and IAG-NH are described. Knowledge of the catalytic mechanism combined with transition state structural information has allowed the design of isozyme-specific, transition state inhibitors that resemble the corresponding enzymatic transition states. The energetic contributions of specific transition state features in each isozyme are further analyzed by comparing the rate effects of inhibitors differing in a single structural feature. Nanomolar inhibitors that are specific for IAG-NH are described, along with others that are specific for IU-NH and some that are potent inhibitors of both isozymes. This advance in inhibitor design may prove to be useful in developing new antiprotozoan agents for disrupting the essential pathways of purine salvage in protozoan parasites.

EXPERIMENTAL PROCEDURES

Enzymes. The nonspecific inosine-uridine nucleoside hydrolase (IU-NH) from *C. fasciculata* was overexpressed in *Escherichia coli* using the pET3d-IUNH expression vector and the purification procedures described previously (10). Purine-specific inosine-adenosine-guanosine nucleoside hydrolase (IAG-NH) from *T. brucei brucei* was overexpressed in *E. coli* using the pET-28a expression vector and was purified as described previously (14).

Iminoribitol Inhibitors. Iminoribitol inhibitors¹ were synthesized by an extension of the methods described earlier for 1-(S)-substituted iminoribitols (16, 17). For each compound, the structure was confirmed by NMR and mass spectrometry. Concentrations of inhibitors were established by ultraviolet absorbance spectra when possible.

Enzymatic Assays. The catalytic activity of IU-NH was measured in reaction mixtures of 1 mL which contained 45–

¹ The nitrogen-substituted ribosyl analogue, 1,4-dideoxy-1,4-imino-D-ribitol, is abbreviated as iminoribitol, and the deoxy compounds are abbreviated as deoxyiminoribitols. Substituted iminoribitols refer to the (1S)-stereochemistry of substituents of the iminoribitol ring. In the paper, numbering in the iminoribitol ring is derived from ribose nucleoside chemistry for the sake of simplicity and consistency. The example for trivial ring numbering is given for **1** in Figure 2. The CAS names for the compounds used here are as follows: **1**, 4-amino-7-[(2S,3S,4R,5R)-3,4-dihydroxy-5-(hydroxymethyl)-2-pyrrolidinyl]-5H-pyrrolo[3,2-*d*]pyrimidine; **2**, [2R-(2 α ,3 β ,4 β ,5 α)]-5-[4-amino-5-(carbonylamino)-3-pyrrolyl]-2-(hydroxymethyl)-3,4-pyrrolidinediol; **3**, [2R-(2 α ,3 β ,4 β ,5 α)]-5-(4-amino-1-naphthalenyl)-2-(hydroxymethyl)-3,4-pyrrolidinediol; **4**, [2R-(2 α ,3 β ,4 β ,5 α)]-5-(5,6-diamino-3-pyridinyl)-2-(hydroxymethyl)-3,4-pyrrolidinediol; **5**, 7-[(2R,4S,5R)-4-hydroxy-5-(hydroxymethyl)-2-pyrrolidinyl]-1,5-dihydro-4H-pyrrolo[3,2-*d*]pyrimidin-4-one; **6**, 2-amino-7-[(2R,4S,5R)-4-hydroxy-5-(hydroxymethyl)-2-pyrrolidinyl]-1,5-dihydro-4H-pyrrolo[3,2-*d*]pyrimidin-4-one; **7**, 7-[(2S,3S,4R,5R)-3,4-dihydroxy-5-methyl-2-pyrrolidinyl]-1,5-dihydro-4H-pyrrolo[3,2-*d*]pyrimidin-4-one; **8**, 7-[(2S,3S,4R,5R)-3,4-dihydroxy-5-(fluoromethyl)-2-pyrrolidinyl]-1,5-dihydro-4H-pyrrolo[3,2-*d*]pyrimidin-4-one; **9**, 9-[[[(2S,3S,4R,5R)-3,4-dihydroxy-5-(hydroxymethyl)-2-pyrrolidinyl]methyl]-1,7-dihydro-6H-purine-6-one]; **10**, 2-amino-9-[[[(2S,3S,4R,5R)-3,4-dihydroxy-5-(hydroxymethyl)-2-pyrrolidinyl]methyl]-1,7-dihydro-6H-purine-6-one]; **11**, 9-[[[(2S,3S,4R,5R)-3,4-dihydroxy-5-(hydroxymethyl)-2-pyrrolidinyl]methyl]-1H-purin-6-amine]; **12**, 1-[[[(2S,3S,4R,5R)-3,4-dihydroxy-5-(hydroxymethyl)-2-pyrrolidinyl]methyl]-1H-purine]; **13**, 7-[(2S,3S,4R,5R)-3,4-dihydroxy-5-(hydroxymethyl)-2-pyrrolidinyl]-1,5-dihydro-4H-pyrrolo[3,2-*d*]pyrimidin-4-one (registry number 209799-67-7); **14**, 2-amino-7-[(2S,3S,4R,5R)-3,4-dihydroxy-5-(hydroxymethyl)-2-pyrrolidinyl]-1,5-dihydro-4H-pyrrolo[3,2-*d*]pyrimidin-4-one (registry number 209799-75-7); **15**, 2-(methylthio)-7-[(2S,3S,4R,5R)-3,4-dihydroxy-5-(hydroxymethyl)-2-pyrrolidinyl]-1,5-dihydro-4H-pyrrolo[3,2-*d*]pyrimidin-4-one; and **16**, [2R-(2 α ,3 β ,4 β ,5 α)]-5-[5-(carbonylamino)-2-pyridinyl]-2-(hydroxymethyl)-3,4-pyrrolidinediol. Compounds **17–20** are described by their trivial names: **17**, 9-deazaadenosine; **18**, 3-deazaadenosine; **19**, 7-deazaadenosine; and **20**, formycin B.

50 mM Hepes (pH 8.0) and either *p*-nitrophenyl β -D-ribofuranoside (53 μ M) or inosine (80 μ M). Chemical synthesis of *p*-nitrophenyl β -D-ribofuranoside has been described previously (6). The reaction was monitored by the formation of *p*-nitrophenylate anion at 400 nm (millimolar extinction coefficient of 15.3 cm^{-1}) or by the difference in ultraviolet absorbance at 280 nm for the production of hypoxanthine (millimolar extinction coefficient of -0.92 cm^{-1}). The extent of hypoxanthine formation was also measured at 293 nm in a coupled assay using xanthine oxidase to form uric acid (millimolar extinction coefficient of 12.9 cm^{-1}) (18). After equilibration at 30 $^{\circ}\text{C}$, the reactions were initiated with sufficient enzyme to produce an optical absorbance change of 0.002–0.020 min^{-1} .

Inhibition Constants. Inhibitors which demonstrated no time-dependent onset of inhibition were assumed to be competitive inhibitors by virtue of their similarity to substrate for these single-substrate hydrolytic enzymes. Determination of initial reaction rates with several inhibitor concentrations gave inhibition curves which were fit to the equation $1/v = 1/k_{\text{cat}} + (K_{\text{m}}/k_{\text{cat}}A)(1 + I/K_{\text{i}})$, where v is the initial rate of product formation, K_{i} is the dissociation constant for the inhibitor, and A , I , K_{m} , and k_{cat} are the substrate concentration, inhibitor concentration, Michaelis constant, and catalytic turnover number, respectively. This method provides accurate dissociation constants for inhibitors that are competitive with substrate and are rapidly reversible relative to the time scale of catalysis. Inhibition constants for novel inhibitors with limited availability were first screened at an inhibitor concentration of 10 μ M with a low substrate concentration. If no inhibition was detected, the level of inhibition is reported as a K_{i} of >30 or $>50 \mu\text{M}$ depending on the assay conditions. Full inhibition analysis was carried out for readily available inhibitors.

Slow-Onset Inhibition Constants. Inhibitors exhibiting slow-onset properties are characterized by an initial time-dependent and a later time-independent inhibition constant (19). Progress curves for compounds exhibiting both inhibitory phases within the time scale of the assay (minutes) were fit to the equation describing slow-onset inhibition, $P = v_{\text{s}}t(v_0 - v_{\text{s}})(1 - e^{-kt})/k$, where P is the product concentration, v_0 is the initial reaction rate, v_{s} is the final steady-state rate, t is time, and k is the first-order rate constant for the slow-onset phase of inhibition. Properties for slow-onset inhibitors can vary greatly, but the compounds used in these assays demonstrated complete onset within 5–10 min. These experiments directly determined v_0 and v_{s} for each inhibitor concentration. Inhibition constants were then derived from plots of v_0 or v_{s} as a function of inhibitor concentration by curve fitting using the expressions $v_0 = (k_{\text{cat}}A)/[K_{\text{m}}(1 + I/K_{\text{i}}) + A]$ in which K_{i} represents the binding constant for the initial, rapidly reversible inhibitor–enzyme association prior to onset and $v_{\text{s}} = (k_{\text{cat}}A)/[K_{\text{m}}(1 + I/K_{\text{i}}^*) + A]$ in which K_{i}^* represents the final, steady state inhibition constant after the slow-onset phase. Detailed examples of this analysis can be found in recent publications (18, 20).

RESULTS AND DISCUSSION

Structural Elements of IU-Nucleoside Hydrolase in a Complex with a Transition State Analogue. Design of inhibitors has been aided by the X-ray crystal structure of

IU-NH from *C. fasciculata* with bound (1*S*)-1-(*p*-aminophenyl)-1,4-dideoxy-1,4-imino-D-ribitol (pAPIR) (12, 13). The structure established the location of a tightly bound calcium ion in the catalytic site that functions to organize the water nucleophile and the ribosyl analogue of the transition state inhibitor. The bound calcium ion has a typical eight-member coordination sphere of oxygen atoms contributed by the 2'- and 3'-hydroxyls of the inhibitor, the water molecule, and amino acids Asp10, Asp15 (bidentate), Thr126, and Asp242 (Figure 1). Enzymatic contacts with the sugar moiety include hydrogen bonds with the imino nitrogen and with all three hydroxyls. The 2'- and 3'-hydroxyls hydrogen bond to Asp14 and Asp242 with crystallographic distances of 2.8 and 2.6 Å, respectively. The hydrogen bond between Glu166 and the 5'-hydroxyl (2.5 Å) positions the 5'-hydroxyl group in an unusual syn geometry, 2.7 Å from the imino nitrogen. The ordered water molecule is coordinated to the Ca^{2+} (2.4 Å), and is hydrogen bonded to Asn168 (2.5 Å) and Asp10 (2.9 Å). These three interactions orient the water oxygen for nucleophilic attack at the ribosyl 1'-carbon of the enzyme-stabilized ribooxocarbenium ion at the transition state. The claim that this complex resembles the transition state is supported by the similar pH profiles for catalysis (k_{cat}) and pAPIR binding (21). Both of these pH profiles differ from the pH dependence of substrate binding. Thus, pAPIR interacts with the same groups that are involved in catalysis, which supports the proposal that it binds as a transition state analogue inhibitor.

In contrast to the many close interactions surrounding the water molecule and the ribosyl analogue, the leaving group contacts are weak and primarily hydrophobic. The leaving group pocket is bounded by two hydrophobic residues, Ile81 and Phe167, and the nearest contact to the phenyl ring is with His82 (3.6 Å). Large conformational changes (up to 25 Å) are evident in this pocket when the empty enzyme is compared to the complex with the bound transition state analogue (12, 13). Information about interactions between the leaving group pocket and the natural substrates is difficult to extract from these two structures due to significant structural differences between the pAPIR inhibitor and a purine/pyrimidine nucleoside, particularly in the base moiety. Activation of the leaving group assists hydrolysis of natural heterocycles even though IU-NH can vigorously hydrolyze *p*-nitrophenyl β -D-ribofuranoside with little apparent need for leaving group assistance. Protonation of N7 by His241 is the most probable mechanism for accomplishing this assistance for purine substrates. The mutant His241Ala decreases k_{cat} by 1000-fold for inosine hydrolysis but does not decrease the extent of catalysis of *p*-nitrophenyl β -D-ribofuranoside (10). The mechanism of leaving group assistance for IU-NH-catalyzed hydrolysis of the more chemically robust pyrimidine nucleosides remains unknown.

The discovery of purine-specific nucleoside hydrolases (GI-nucleoside hydrolase and IAG-nucleoside hydrolase) revealed surprising differences in sequence and catalytic properties compared to those of the nonspecific nucleoside hydrolase, IU-NH (4, 5, 14). Although amino acids in contact with the calcium and sugar hydroxyls are highly conserved, the leaving group pocket sequences differ. This difference is consistent with the additional leaving group activation evident in purine-specific enzymes (6, 14), and the slow hydrolysis of *p*-nitrophenyl β -D-ribofuranoside (10^{-4} times

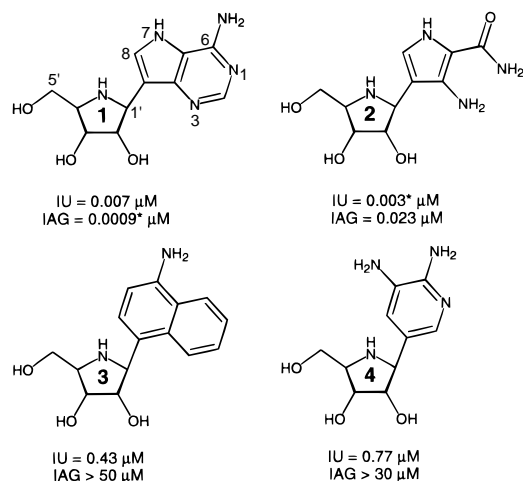


FIGURE 2: Iminoribitol analogues with structural and hydrophobic differences in the carbon-bonded leaving group substituents. The descriptions IU and IAG refer to dissociation constants for IU-NH and IAG-NH determined as described in Experimental Procedures. The values for inhibition of IAG-NH by **1** and of IU-NH by **2** are K_i^* values, where the values of K_i were 3 and 6 nM, respectively. The dissociation constants for **3** and **4** are K_i values. Standard errors were determined for all inhibition constants and were on average $\pm 10\%$ of the dissociation constants. All errors of the K_i values were within $\pm 20\%$ of the values.

that with IU-nucleoside hydrolase). Poor hydrolysis of this unnatural substrate is now considered a chemical hallmark for the presence of significant leaving group activation in ribohydrolases (6). Additional support for this mechanism for IAG-NH comes from pH studies of k_{cat} , where the highest activity is at acidic pH as a result of the protonation of two enzymatic groups which is required to form fully active enzyme (5). In contrast, the IU-NH employs acid–base catalysis with one acidic and one basic group in the k_{cat} profile (11).

On the basis of this mechanistic information, compounds **1–20** were prepared and tested as inhibitors of IU-NH from *C. fasciculata* and of IAG-NH from *T. brucei brucei*. These iminoribitol nucleosides were designed to recognize catalytic interactions, some common to both isozyme transition states and some specific to one or the other. Both general and specific inhibitors would be desirable, and the isozyme specificity of the inhibitors will be emphasized here.

Size and Shape of the Leaving Group. The hypotheses to be tested with inhibitors **1–4** are as follows. (1) Good inhibitors of IU-NH require an iminoribitol sugar analogue and prefer a hydrophobic aglycon similar in size to a purine or pyrimidine base, whereas (2) good inhibitors of IAG-NH prefer an iminoribitol sugar but require a base analogue with a rigid purine pattern of H-bonding partners (Figure 2). Compound **1** features, in addition to the iminoribitol, the same H-bond pattern in the pyrimidine ring as adenine and a more basic nitrogen at N7 to act as an improved hydrogen-bond acceptor. Since both isozymes use adenosine as a substrate, **1** might be expected to be a reasonable transition state analogue for both enzymes. In fact, **1** is a powerful inhibitor for both hydrolases, with a K_i of 7 nM for IU-NH and K_i^* of 0.9 nM for IAG-NH. This is 4 times tighter than that of the previous best iminoribitol inhibitor for IU-NH, (1*S*)-1-(*p*-bromophenyl)-1,4-dideoxy-1,4-imino-D-ribose, with a K_i of 28 nM and 2000 times tighter than the previous record

holder for IAG-NH, 3-deazaadenosine, with a K_i of 1.8 μ M (5, 11). Compound **1** is a slow-onset inhibitor for IAG-NH (pre-steady state K_i of 3 nM) and binds with sufficient affinity to have potential as a physiologically effective antibiotic.

Elimination of C2 from **1** and oxo substitution at C6 give **2**. Rotational freedom of the carboxamide permits a hydrogen-bonding pattern similar to that of **1**, but the exocyclic amino group of **1** can only function as a hydrogen-bond donor. This change decreases inhibitor affinity for IAG-NH ($K_i = 23$ nM for **2**) but improves binding to IU-NH and also changes the kinetics of inhibition. Compound **2** exhibits slow-onset inhibition (initial $K_i = 6$ nM; final $K_i^* = 3$ nM) and is the most powerful iminoribitol inhibitor known for IU-NH. The indiscriminating base acceptance of IU-NH is highlighted by the aminonaphthyl iminoribitol **3**, which efficiently inhibits the enzyme ($K_i = 0.43 \mu$ M). Since unsubstituted iminoribitol binds IU-NH with a K_i of 10 μ M (9), the hydrophobic group contributes a factor of 20 to the binding affinity. As expected, IAG-NH is not as tolerant of base variations. The slight increase in size and the lack of ring nitrogens in **3** resulted in no detectable inhibition when it was tested at 10 μ M. The diaminopyridyl derivative **4** also binds poorly to purine-specific IAG-NH. A favorable alignment of potential hydrogen-bonding groups on the base with complementary groups on the enzyme is evidently not possible. Predictably, the hydrophobic properties of **4** permit it to bind well to IU-NH ($K_i = 0.77 \mu$ M).

2'- and 5'-Deoxyiminoribitols. The hypotheses to be tested with compounds **5–8** are as follows. (1) Inhibition of IU-NH is sensitive to iminoribitol alteration because of a strong preference for ribosyl substrates and because transition state interactions are concentrated primarily on the sugar, and (2) inhibition of IAG-NH is more tolerant of sugar changes because substrate and transition state interactions are focused more on the base. The reference compound for this inhibitor series is 9-deazahypoxanthine iminoribitol (**13**), a potent inhibitor of both IU-NH ($K_i = 42$ nM) and IAG-NH ($K_i = 24$ nM). Formal substitution of the 2'-hydroxyl with hydrogen (**5**) dramatically decreases the extent of binding to IU-NH ($K_i > 50 \mu$ M). In contrast to its base permissiveness, IU-NH exhibits a rigid sugar intolerance by insisting on ribosyl nucleosides. Interaction of the sugar 2'-hydroxyl with the catalytic site calcium is essential for both binding and catalysis (for 2'-deoxyinosine, $k_{\text{cat}} < 0.001 \text{ s}^{-1}$ and $K_m = 2$ mM; for inosine, $k_{\text{cat}} = 30 \text{ s}^{-1}$ and $K_m = 0.4$ mM) (3). A much smaller effect is observed on binding of **5** to IAG-NH ($K_i = 0.66 \mu$ M). With this purine-specific hydrolase, the loss of the 2'-hydroxyl is partially overcome by substantial interactions with the 9-deazahypoxanthine leaving group analogue (for 2'-deoxyadenosine, $k_{\text{cat}} = 0.02 \text{ s}^{-1}$ and $K_m = 42 \mu$ M; for adenosine, $k_{\text{cat}} = 34 \text{ s}^{-1}$ and $K_m = 18 \mu$ M) (5). Guanosine is a good substrate for both enzymes, and the inhibition by 9-deazaguanine 2'-deoxyiminoribitol (**6**) follows the same pattern as seen for **5**.

Substrate specificity and kinetic isotope effect studies with IU-NH revealed a 5'-hydroxyl requirement for substrate activity (3). A substantial 5'- ^3H kinetic isotope effect (5.1% with [5'- ^3H]inosine) has been observed at this position, an unexpected and chemically unprecedented remote kinetic isotope effect (8). This observation is thought to result from 5'-hydroxyl anchoring by the enzyme to position the hydroxymethyl in a suitable orientation for the O5' lone pair

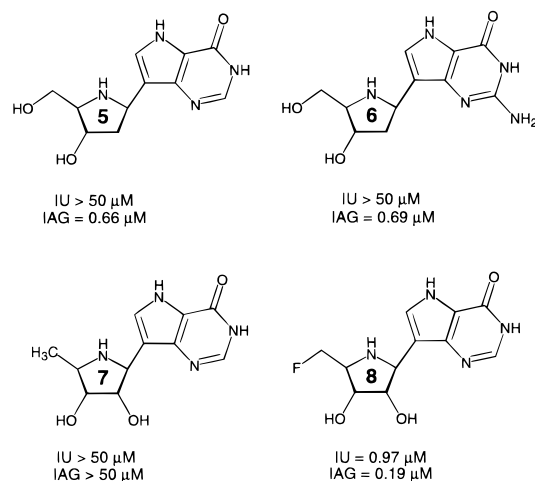


FIGURE 3: Inhibition by deoxyiminoribitol analogues of 9-deazahypoxanthine and 9-deazaguanine. Inhibition constants that are > 50 μ M indicate no detectable inhibition at inhibitor concentrations up to and including 10 μ M. The remainder of the inhibition constants are K_i values, with error limits as described in the legend of Figure 2.

orbitals to interact with the transition state ribooxocarbenium ion (9). This anchoring causes distortion of the 5'-carbon sp^3 geometry, altering the C5'-H vibrational bending modes and generating the kinetic isotope effect. Removal of the 5'-hydroxyl (7) eliminates significant binding ($K_i > 50 \mu$ M) to IU-NH. The crystal structure of IU-NH with bound iminoribitol indicates a short hydrogen bond (2.5 Å) between Glu166 and the 5'-hydroxyl (Figure 1). It is likely that the 5'-hydroxyl-Glu166 interaction enables distortion of the entire sugar, allowing favorable enzyme contacts with the 2'- and 3'-hydroxyls. The 5'-hydroxyl interaction is apparently less essential for IAG-NH than for IU-NH on the basis of the smaller 5'- 3 H kinetic isotope effect (2.7% with [5'- 3 H]inosine)² and the report of a detectable catalytic reaction with 5'-deoxyadenosine ($k_{cat} = 2\%$ of that with adenosine, $K_m = 10$ mM) (5). Nonetheless, the poor binding of 5'-deoxysubstrates is reflected in the failure of IAG-NH to bind tightly to 7 ($K_i > 50 \mu$ M). However, replacement of a 5'-hydrogen in 7 with fluorine (8) partially restores the interaction with both enzymes, clearly illustrating the hydrogen-bonding nature of the 5'-interaction.

Methylene-Bridged Purine Iminoribitols. In the dissociative transition states of IU- and IAG-nucleoside hydrolases, the *N*-glycosyl bond stretches to approximately 2 Å (9).² It is possible that inhibitors with a longer base-sugar distance might bind favorably. A methylene spacer was incorporated to suitably position the purine and iminoribitol moieties (compounds 9–12, Figure 4). The methylene-bridged compounds incorporating purine bases (9–11) are low-micromolar inhibitors of both enzymes ($K_i = 3$ –28 μ M). For IAG-NH, binding constants are generally similar to K_m values for the corresponding purine base substrates (18–46 μ M) and 1 order of magnitude lower than the K_m for IU-NH (380–460 μ M) (3). These inhibitors bind approximately 3 orders of magnitude more weakly than the corresponding 9-deazapurine iminoribitols (1, 13, and 14). This decrease is likely due to secondary changes in purine ring orientation

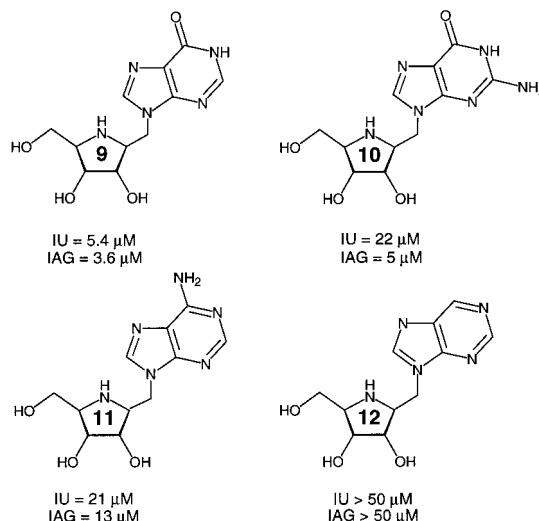


FIGURE 4: Inhibition of nucleoside hydrolases by methylene-bridged purine iminoribitols. The meaning of the kinetic constants is the same as indicated in the legend of Figure 3.

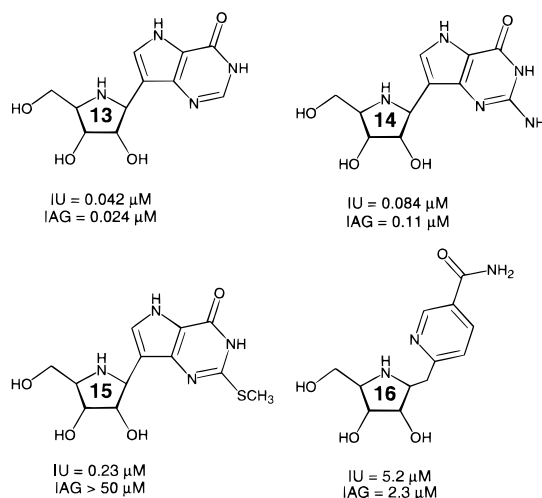


FIGURE 5: Effect of leaving group substituents on the K_i values for iminoribitol inhibitors with IU-NH and IAG-NH. The inhibition constants are all K_i values, determined as described in Experimental Procedures.

with respect to the iminoribitol caused by the methylene bridge, and to the low pK_a at N7 of the natural purine ring (12). No inhibition was detected with the methylene-bridged, purine base derivative 12 at 10 μ M ($K_i > 50 \mu$ M), suggesting that a substantial part of the binding energy for 9–11 may be attributed to deazapurine substituents and not just to the iminoribitol or to the deazapurine ring. Effects of the methylene bridge are best illustrated by comparing 1 and 11, compounds that are isosteric except for the 9-deaza and the CH_2 bridge. These changes decrease the affinity by 770–4000-fold, indicating unfavorable contacts with the adenine ring.

Hydrogen-Bonding Pattern of the Leaving Group. Since inosine and guanosine are good substrates for both IU-NH and IAG-NH, the corresponding 9-deazapurine iminoribitol analogues (compounds 13 and 14, Figure 5) bind both enzymes well, with K_i values that are approximately 1000 times smaller than those of substrates (24–110 nM). The added 2-amino group of 14 compared to 13 slightly decreases the affinity for both enzymes, with a greater effect on IAG-NH inhibition (5-fold decrease). Predictably, increasing the

² D. W. Parkin, A. A. Sauve, P. J. Berti, and V. L. Schramm, unpublished results.

bulk of the 2-substituent (**15**, SCH₃) destroys the affinity for base-specific IAG-NH ($K_i > 50 \mu\text{M}$) while decreasing the affinity for IU-NH less drastically ($K_i = 230 \text{ nM}$). This result highlights the contrast between the stringent leaving group requirements of IAG-NH and the flexible, hydrophobic leaving group requirements of IU-NH. Leaving-group specificity was further probed by replacing the purine leaving group with the methylene-bridged carboxamidopyridine derivative **16**. If catalytic sites are sufficiently flexible around the leaving group, favorable interactions might still be expected with **16** since it contains three potential H-bonding sites and the methylene bridge permits rotational access to a wide range of hydrogen-bonding conformations. The K_i values for IU-NH (5.2 μM) and IAG-NH (2.3 μM) show that such flexibility is limited and corroborate the importance of the spatial pattern of H-bonding sites.

Contribution of Iminoribitol versus Ribose. The transition state for IU-NH has significant ribooxocarbenium ion character. Enzyme residues that permit formation of this high-energy species have been reported to interact with iminoribitol inhibitors through hydrogen bonds to the unprotonated imino group, providing part of the favorable binding energy observed with these proposed transition state analogues (21). The iminoribitol-contacting amino acids are highly conserved between IAG-NH and IU-NH; therefore, it is anticipated that similar enzyme–iminoribitol interactions occur in IAG-NH (5). The relative thermodynamic contribution of these interactions to enzyme transition state stabilization can be estimated by comparing inhibition by **1** with that of the corresponding ribosyl, C-nucleoside, 9-deazaadenosine (**17**). Using the Gibbs free energy expression [$\Delta G = RT \ln(K_{d,\text{imino}}/K_{d,\text{ribose}})$] and substituting the IAG-NH equilibrium dissociation constants of **1** (0.9 nM) and **17** (410 nM) for $K_{d,\text{imino}}$ and $K_{d,\text{ribose}}$, we estimated the iminoribitol contribution to binding is 3.7 kcal/mol more favorable than that of ribose. This is consistent with the presence of an additional hydrogen bond with normal energy, presumably with the nitrogen of the iminoribitol. A similar calculation using the IU-NH inhibition constants for the same pair of compounds (7 nM for **1** and 1.5 mM for **17**) reveals a binding energy contribution of 7.4 kcal/mol from the interaction with the nitrogen atom of the iminoribitol. Binding differences between **1** and **17** can be viewed as an indication of the importance of oxocarbenium ion stabilization at the transition state for each enzyme. The relative contribution of oxocarbenium ion stabilization (3.7 kcal/mol) calculated in this way agrees well with that determined from the activity differences of each isozyme for *p*-nitrophenyl β -D-ribofuranoside (Figure 7). IU-NH contributes 13.1 kcal/mol to the activation energy through ribosyl interactions, while IAG-NH contributes 8.9 kcal/mol from this ribosyl interaction in the transition state. The difference of 4.2 kcal/mol is similar to the energetic difference in the iminoribitol contribution to the binding of inhibitors by these enzymes (7.4 kcal/mol – 3.7 kcal/mol = 3.7 kcal/mol). This relationship is demonstrated in Figure 7.

The ribosyl analogues 3-deazaadenosine (**18**), tubercidin (7-deazaadenosine, **19**), and formycin B (**20**) are poor inhibitors of IU-NH. The same compounds bind with K_i values of 2–59 μM to IAG-NH, a range of dissociation constants similar to those of substrates for this enzyme. The ribosyl groups of **17**–**20** make them analogues of the

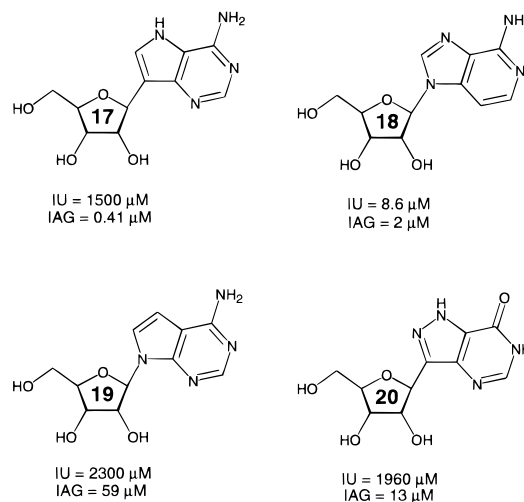


FIGURE 6: Inhibition of IU-NH and IAG-NH by ribosyl analogues of the substrates and transition state analogue inhibitors. The inhibition constants for IAG-NH were taken from ref 5 and those for IU-NH with compounds **19** and **20** from ref 5. The others were determined in this study.

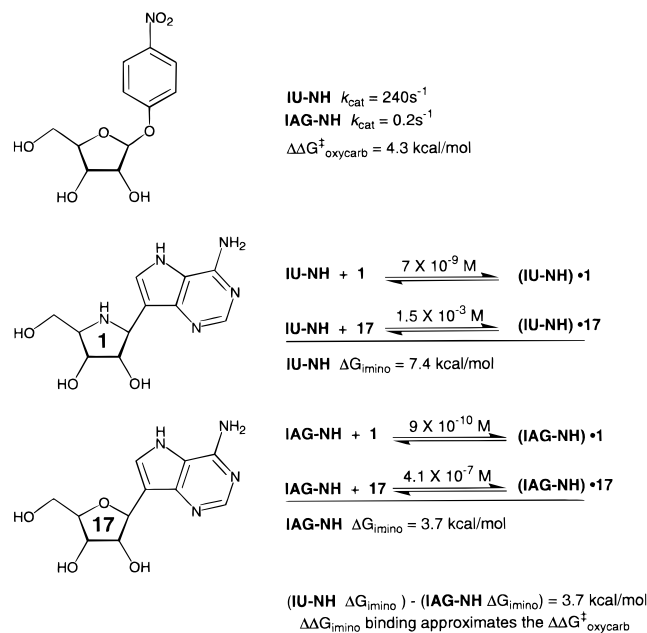
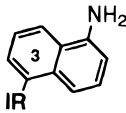
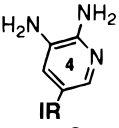
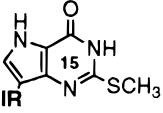
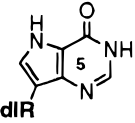
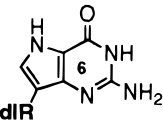
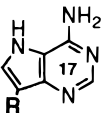
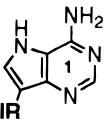
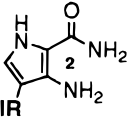
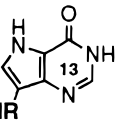
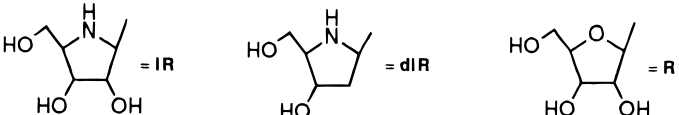


FIGURE 7: Thermodynamic contribution of the iminoribitol group to catalysis and inhibitor binding from isosteric inhibitor studies. The upper panel demonstrates the difference in catalytic efficiency for the substrate *p*-nitrophenyl β -D-ribofuranoside with IU-NH and IAG-NH, reflecting the difference in the ability of the enzymes to form the reactive ribooxocarbenium ion transition state. The dissociation constants for **1** and **17** from complexes of IU-NH and IAG-NH establish the energy associated with interactions involving the imino group since the inhibitors are otherwise isosteric. This specific interaction contributes 7.4 kcal/mol more to the binding of **1** than of **17** for IU-NH. This interaction contributes 3.7 kcal/mol more to the binding of **1** than of **17** for IAG-NH. The difference in catalytic efficiency for *p*-nitrophenyl β -D-ribofuranoside between the two enzymes can be attributed almost exclusively to the transition state stabilization of a stronger interaction with the ribooxocarbenium ion.

Michaelis complex and fail to capture transition state interactions for either enzyme. It is interesting to note that the binding affinity of IAG-NH for **17**, **18**, and **20** seems to depend on the $\text{p}K_{\text{a}}$ of N7.

Table 1: Inhibitor Specificity for Nucleoside Hydrolase Isozymes

Inhibitors	nM dissociation constants	
IU-NH-specific inhibitors ^a	IU-NH	IAG-NH
	430	>50,000 ^d
	770	>30,000
	230	>50,000
IAG-NH-specific inhibitors ^b		
	>50,000 ^d	660
	>50,000	690
	1,500,000	410
broad specificity inhibitors ^c		
	7	0.9
	3	23
	42	24
		

^a Inhibitors that bind >100-fold more tightly to IU-NH than to IAG-NH. All inhibitors are assumed to be competitive inhibitors with respect to substrate. ^b Inhibitors that bind >100-fold more tightly to IAG-NH than to IU-NH. ^c Inhibitors binding more tightly than 100 nM to both enzymes. ^d Less than 10% inhibition at 10 μ M inhibitor. Depending on substrate concentration, the level of detection indicates a lower limit for the inhibition constant.

CONCLUSIONS

Catalysis of *N*-glycosyl hydrolysis of purine nucleosides by nucleoside hydrolases proceeds through a dissociated,

S_N1-like transition state and can employ three chemical strategies: (1) leaving group activation by protonation or hydrogen bonding to the purine leaving group, (2) formation of a ribooxocarbenium ion by distortion and electrostatic

stabilization of the ribosyl group, and (3) activation and strategic positioning of a water molecule for capturing the ribooxocarbenium ion at the transition state.

Of the three chemical strategies for catalysis listed above, only two were employed here for inhibitor design. Mimicry of the attacking water hydroxyl is not required for good inhibition. Water from solvent is available to occupy this site and out of necessity binds prior to inhibitor since the water-binding site is not accessible to bulk solvent in the bound complex. Crystallography of unliganded IU-NH and of the enzyme complexed with inhibitor establishes the presence of a bound water in this site (12, 13). KIE studies of inosine hydrolysis catalyzed by IU-NH indicate that the calcium-bound water is not significantly bonded to C1' at the transition state. Therefore, accessing purine and ribosyl transition state activation forces in an inhibitor-enzyme interaction is the main design goal. All effective inhibitors for nucleoside hydrolase enzymes include an iminoribitol as the ribooxocarbenium ion mimic, leaving manipulations in the sugar hydroxyls and the aglycon as the primary means of obtaining specificity in both IU-NH and IAG-NH.

Specific inhibition of isozymes is not a trivial goal. Information from X-ray crystal structures and gene sequence comparison indicate that water activation by Ca^{2+} is similar for both nucleoside hydrolases, and KIE studies indicate a general structural likeness between the two transition states.² Therefore, the only major characteristic differentiating these isozymes is the relative emphasis on leaving group activation compared to ribosyl activation. This feature can be used to design isozyme-specific inhibitors by manipulating the different ribosyl and/or leaving group interactions. The best results for inhibitors designed in this way are shown in Table 1 and are divided into three classes: (1) IU-NH-specific, (2) IAG-NH-specific, and (3) nonspecific, with inhibition of both isozymes.

From these data, the following generalizations can be made. For good IU-NH inhibitors, a hydrophobic, planar leaving group is necessary, with or without hydrogen-bonding sites and roughly similar in size to purine or pyrimidine. For specific IU-NH inhibition, the leaving group should be incompatible with the purine-binding pocket of IAG-NH, either in size or by the elimination of the heterocyclic nitrogens. In the case of IAG-NH, good inhibition requires a minimal difference in the base mimic from the hydrogen-bonding pattern of natural aglycons hypoxanthine, adenine, and guanine. Elevating the pK_a of N7 (as in the case of 9-deazapurines) also is important.³ The stringent purine requirement is consistent with leaving group activation being a major force in stabilizing the transition state of IAG-NH. For specific IAG-NH inhibitors, modifications in the ribooxocarbenium ion analogue should be used. The tolerance of IAG-NH to changes in the iminoribitol compared with the striking sensitivity of IU-NH to such variations is consistent with the relatively greater importance of leaving group interactions in the base-specific isozyme and of ribooxocarbenium interactions in the non-base-specific isozyme (6).

Inhibitors capable of effectively binding to either isozyme are the most powerful. They take advantage of transition state features common to both IU-NH and IAG-NH. In particular, hydrogen-bonding sites are patterned like natural purine leaving groups, and the iminoribitol ribooxocarbenium mimic includes a full complement of exocyclic hydroxyls. Research on such broad-spectrum inhibitors is important because physiological disruption of the protozoan purine-salvage pathway, upon which all protozoan parasites are dependent for survival, will likely require inhibition of all hydrolase isozymes. Complete inhibition of purine salvage pathways has not been easy to achieve, because expression of more than one isozyme is common in most well-characterized organisms (e.g., refs 4 and 5). In addition, powerful, broad-specificity inhibitors (typified by **1**) may be useful in testing nucleoside hydrolases as targets for specific antiprotozoan agents. The results summarized here demonstrate the feasibility of producing broad-spectrum antiprotozoal agents from the catalytic mechanisms of nucleoside hydrolase isozyme inhibitors.

REFERENCES

- Berens, R. L., Marr, J. J., LaFon, S. W., and Nelson, D. J. (1981) *Mol. Biochem. Parasitol.* **3**, 187–196.
- Berens, R. L., Krug, E. C., and Marr, J. J. (1995) in *Biochemistry and Molecular Biology of Parasites* (Marr, J. J., and Müller, M., Eds.) pp 89–117, Academic Press, New York.
- Parkin, D. W., Horenstein, B. A., Abdulah, D. R., Estupiñán, B., and Schramm, V. L. (1991) *J. Biol. Chem.* **266**, 20658–20665.
- Estupiñán, B., and Schramm, V. L. (1994) *J. Biol. Chem.* **269**, 23068–23073.
- Parkin, D. W. (1996) *J. Biol. Chem.* **271**, 21713–21719.
- Mazzella, L. J., Parkin, D. W., Tyler, P. C., Furneaux, R. H., and Schramm, V. L. (1996) *J. Am. Chem. Soc.* **118**, 2111–2112.
- Schramm, V. L. (1997) *Curr. Opin. Chem. Biol.* **1**, 323–331.
- Horenstein, B. A., Parkin, D. W., Estupiñán, B., and Schramm, V. L. (1991) *Biochemistry* **30**, 10788–10795.
- Horenstein, B. A., and Schramm, V. L. (1993) *Biochemistry* **32**, 7089–7097.
- Gopaul, D. N., Meyer, S. L., Degano, M., Sacchettini, J. C., and Schramm, V. L. (1996) *Biochemistry* **35**, 5963–5970.
- Parkin, D. W., Limberg, G., Tyler, P. C., Furneaux, R. H., Chen, X.-Y., and Schramm, V. L. (1997) *Biochemistry* **36**, 3528–3534.
- Degano, M., Almo, S., Sacchettini, J. C., and Schramm, V. L. (1998) *Biochemistry* **37**, 6277–6285.
- Degano, M., Gopaul, D. N., Scapin, G., Schramm, V. L., and Sacchettini, J. C. (1998) *Biochemistry* **37**, 5971–5981.
- Pellé, R., Schramm, V. L., and Parkin, D. W. (1998) *J. Biol. Chem.* **273**, 2118–2126.
- Bagdassarian, C. K., Schramm, V. L., and Schwartz, S. D. (1996) *J. Am. Chem. Soc.* **118**, 8825–8836.
- Horenstein, B. A., Zabinski, R. F., and Schramm, V. L. (1993) *Tetrahedron Lett.* **34**, 7213–7216.
- Furneaux, R. H., Limberg, G., Tyler, P. C., and Schramm, V. L. (1997) *Tetrahedron* **53**, 2915–2930.
- Miles, R. W., Tyler, P. C., Furneaux, R. H., Bagdassarian, C. K., and Schramm, V. L. (1998) *Biochemistry* **37**, 8615–8621.
- Morrison, J. F., and Walsh, C. T. (1988) *Adv. Enzymol. Relat. Areas Mol. Biol.* **61**, 201–301.
- Li, C. M., Tyler, P. C., Furneaux, R. H., Kicska, G., Xu, Y., Grubmeyer, C., Girvin, M. E., and Schramm, V. L. (1999) *Nat. Struct. Biol.* (in press).
- Parkin, D. W., and Schramm, V. L. (1995) *Biochemistry* **34**, 13961–13966.

BI990829U

³ The absolute requirement for exocyclic substituents is uncertain, and the inhibition properties of 9-deazapurine iminoribitol have not yet been explored.